Supplementary Information

Investigation of the interface structure and electronic state of nanocomposite $La_{0.6}Sr_{0.4}Co_{0.2}Fe_{0.8}O_{3-\delta}$ and $Ce_{0.9}Gd_{0.1}O_{2-\delta}$ electrode for solid oxide fuel cells

Daisuke Asakura,*[a] Tomohiro Ishiyama,*[a] Eiji Hosono,[a] Katherine Develos-Bagarinao,[b] Katsuhiko Yamaji,[a] Masaki Kobayashi,[c,d] Miho Kitamura,[e,f] Koji Horiba,[e,f] and Haruo Kishimoto[b]

[a]*Research Institute for Energy Efficient Technologies, National Institute of Advanced Industrial Science and Technology (AIST), 1-1-1 Higashi, Tsukuba, Ibaraki 305-8565, Japan*
[b]*Global Zero Emission Research Center, National Institute of Advanced Industrial Science and Technology (AIST), 16-1 Onogawa, Tsukuba, Ibaraki 305-8569, Japan*
[c]*Center for Spintronics Research Network, The University of Tokyo, 7-3-1 Hongo, Bunkyo-ku, Tokyo 113-8656, Japan*
[d]*Department of Electrical Engineering and Information Systems, The University of Tokyo, 7-3-1 Hongo, Bunkyo-ku, Tokyo 113-8656, Japan*
[e]*NanoTerasu Center, National Institutes for Quantum Science and Technology (QST), 6-6-11-901 Aoba, Aramaki, Aoba-ku, Sendai, Miyagi 980-8579, Japan*
[f]*Photon Factory, Institute of Materials Structure Science, High Energy Accelerator Research Organization (KEK), 1-1 Oho, Tsukuba, Ibaraki 305-0801, Japan*

Number of oxygen atoms in LSCF and GDC interface

The possible oxygen coordination sites are visualized using structural models. The oxygen atoms highlighted in yellow indicate the same positions in both (a) and (b). A surface structure in which an additional oxygen-only layer is added to the AO plane for LSCF. The number of oxygen atoms on the AO-terminated surface of the LSCF phase and on the terminated surface of the GDC phase is equivalent.

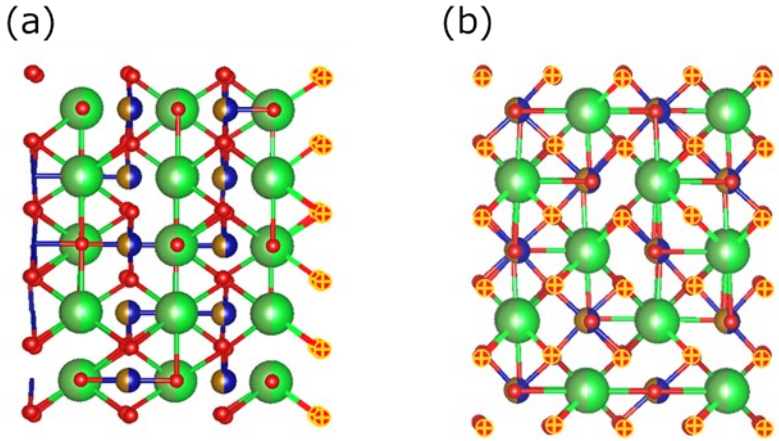

Fig. S1 Atomic model of LSCF viewed along the (a) [2-10] and (b) [012] projection directions.

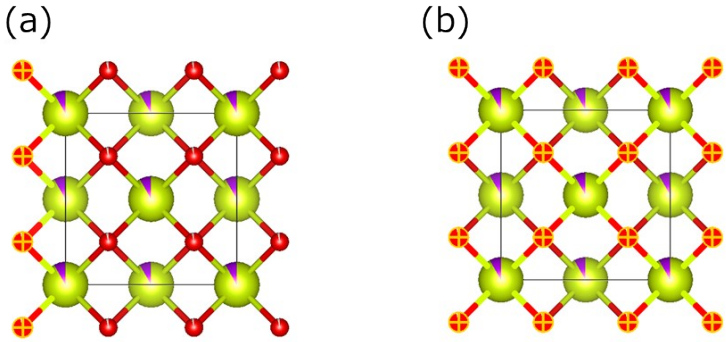

Fig. S2 Atomic model of GDC viewed along the (a) [100] and (b) [010] projection directions.

CTM calculation for Fe^{4+} states

To explain the Fe $L_{2,3}$-edge TEY XAS line shape of the nanocomposites, we also performed CTM calculation for Fe^{4+} states. Figure S3 shows two examples (the electronic structure parameters are summarized in Table S1) for Fe^{4+} states, the calculation for the Fe^{3+} state (ii) determined in the text, and the experimental spectrum of the nanocomposite (grown at 750 ∘C). For both cases of the Fe^{4+} states, the main peak positions for the L_3 and L_2 regions are clearly different from the experiment and calculation for the Fe^{3+} state. Therefore, the Fe $L_{2,3}$-edge TEY XAS of the nanocomposites does not involve Fe^{4+} states.

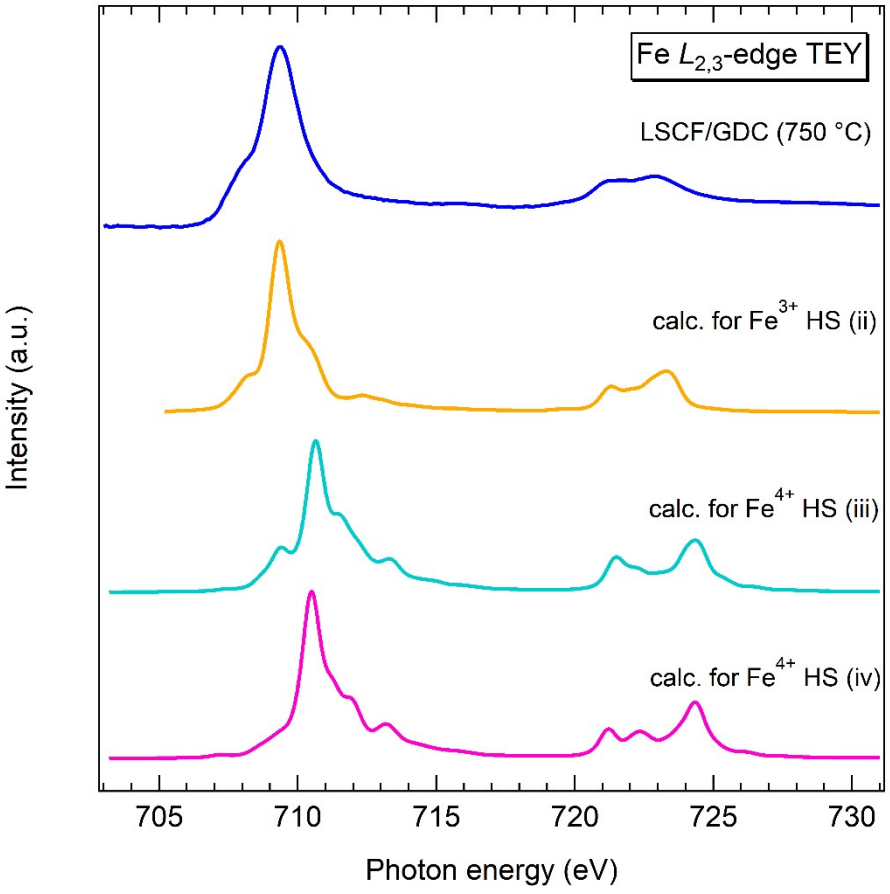

Fig. S3 Examples of CTM calculation for Fe^{4+} states with the Fe $L_{2,3}$-edge TEY XAS result of the LSCF/GDC nanocomposite (750 ∘C) and CTM calculation for the Fe^{3+} states in the text.

Table S1 Electronic structure parameters used for the Fe^{4+} calculations (Fig. S3).

	Fe^{4+} HS (iii)	Fe^{4+} HS (iv)
$10Dq$	1.0	0.5
U	5.0	5.0
Q	6.0	6.0
Δ	2.0	2.0

Fe $L_{2,3}$-edge PFY XAS

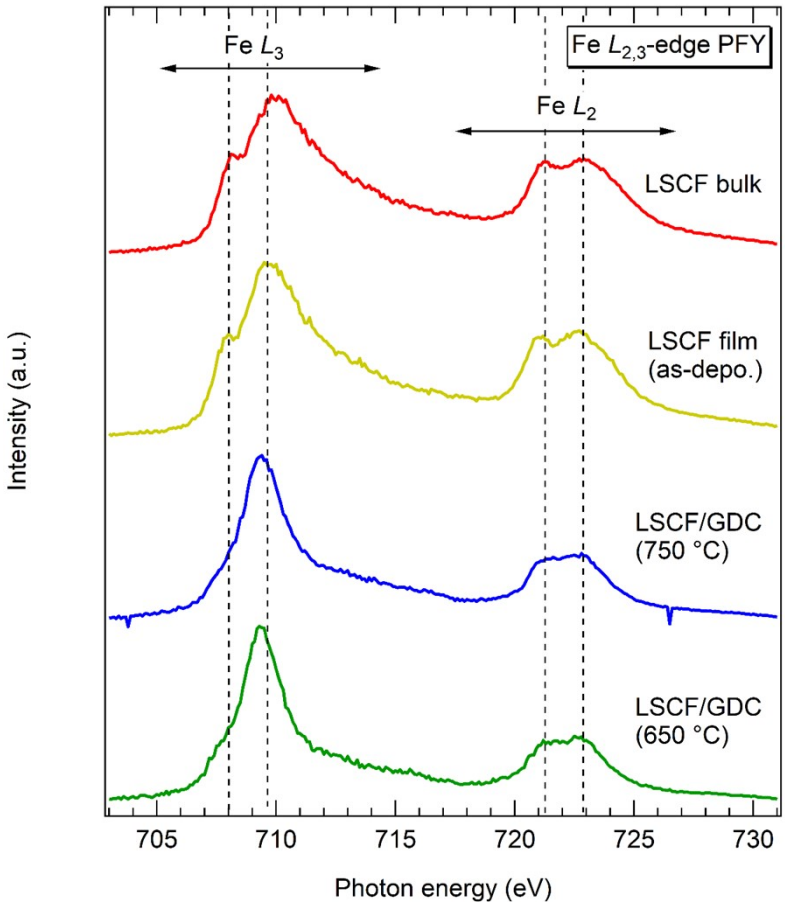

Fig. S4 Fe $L_{2,3}$-edge PFY XAS spectra for the LSCF bulk, as-deposited film, and nanocomposites.

Co L_3-edge TEY XAS of LSCF bulk and as-deposited film

Figure S5 shows the magnified Co L_3-edge TEY XAS spectra for the LSCF bulk and LSCF as-deposited film. For the LSCF as-deposited film, the peak-top position shifts to higher energy side by ~0.2 eV (as the black arrows indicate), and the shoulder structure centered at ~781 eV is higher (as the green arrows) than that for the LSCF bulk. These differences suggest that the LSCF as-deposited film includes some Co^{4+} low-spin-state components as discussed in the text. The enhancement for 776-779 eV in the spectrum of the LSCF as-deposited film is attributed to Co^{2+} high-spin-state component.

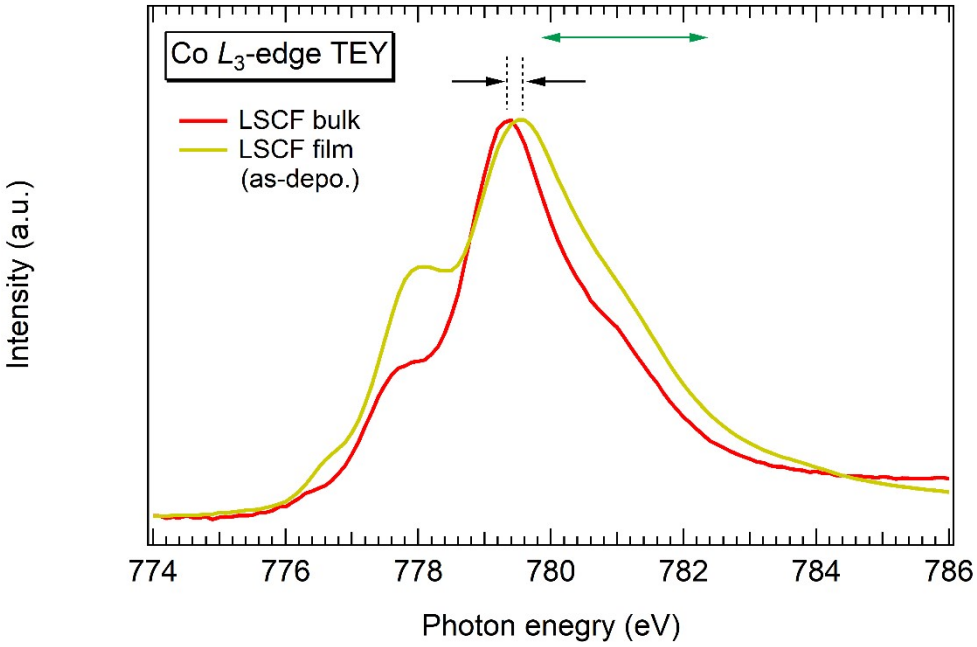

Fig. S5 Co L_3-edge TEY XAS spectra for the LSCF bulk and as-deposited film. The spectra are normalized at the peak top.

Co $L_{2,3}$-edge PFY XAS

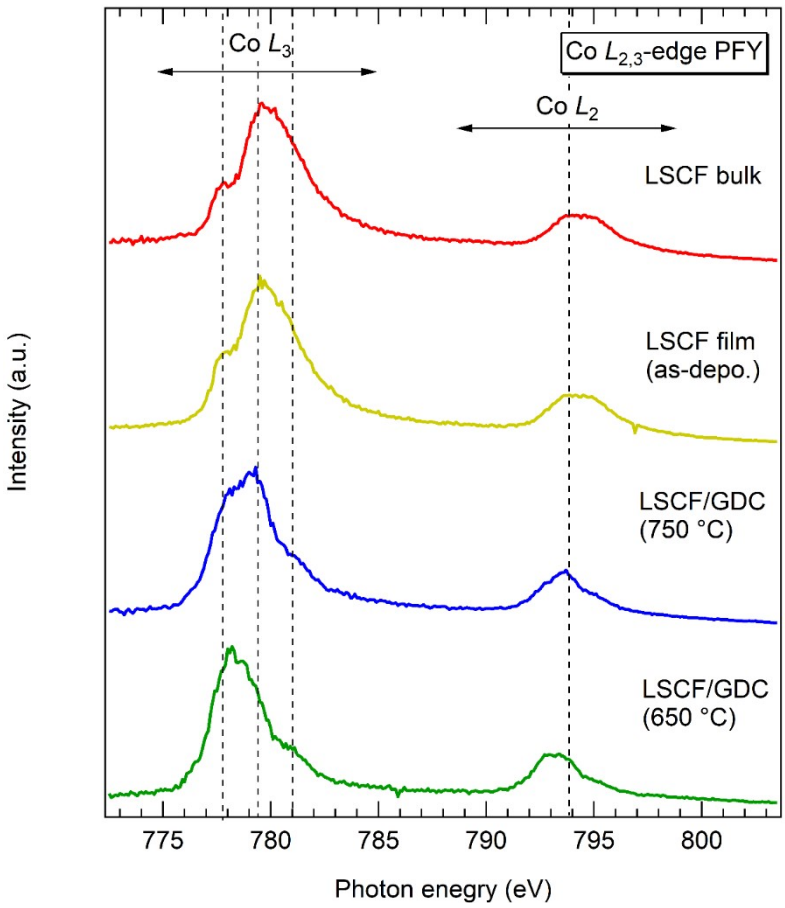

Fig. S6 Co $L_{2,3}$-edge PFY XAS spectra for the LSCF bulk, as-deposited film, and nanocomposites.

Ce $M_{4,5}$-edge TEY XAS

The Ce $M_{4,5}$-edge (3*d*-4*f* absorption) TEY XAS of the nanocomposites were performed to reveal the Ce 4*f* electronic structure of the GDC layers. Figure S4 shows the results with those of GDC bulk and GDC film as reference samples. The line shapes of all the spectra are similar to those in previous reports of CeO_2 series [S1-S4], suggesting that the valence of Ce is close to 4+. Thus, the Ce 4*f* electronic structure is almost unchanged for the nanocomposites. On the other hand, the M_5/M_4 peak-area ratio of the GDC thin film is larger than those of the others. This result indicates that the Ce of the GDC thin film is slightly reduced [S1].

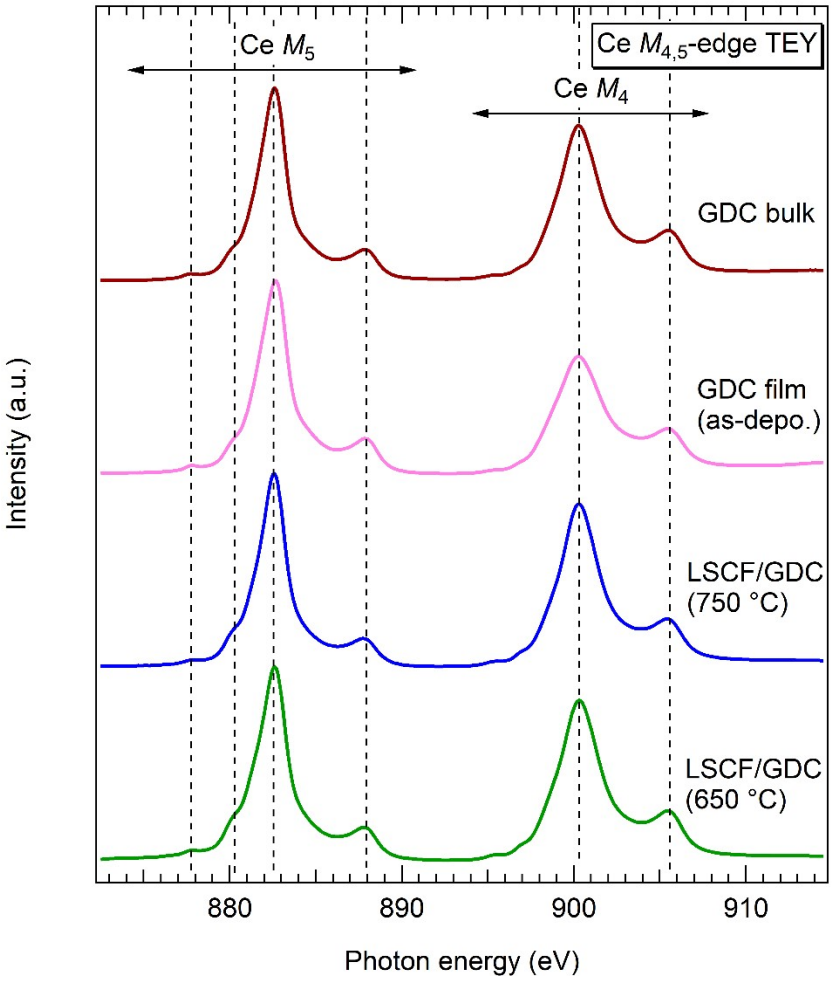

Fig. S7 Ce $M_{4,5}$-edge TEY XAS spectra for the LSCF bulk, as-deposited LSCF film, and LSCF/GDC nanocomposites.

References

[S1] L. Wu, H. J. Wiesmann, A. R. Moodenbaugh, R. F. Klie, Y. Zhu, D. O. Welch, and M. Suenaga, *Phys. Rev. B,* 2004, **69**, 125415.

[S2] C. Mitra, Z. Hu, P. Raychaudhuri, S. Wirth, S. I. Csiszar, H. H. Hsieh, H.-J. Lin, C. T. Chen, and L. H. Tjeng, *Phys. Rev. B,* 2003, **67**, 092404.

[S3] S. M. Butorin, D. C. Mancini, J.-H. Guo, N. Wassdahl, J. Nordgren, M. Nakazawa, S. Tanaka, T. Uozumi, A. Kotani, Y. Ma, K. E. Myano, B. A. Karlin, and D. K. Shuh, *Phys. Rev. Lett.*, 1996, **77**, 574-577.

[S4] S. G. Minasian, E. R. Batista, C. H. Booth, D. L. Clark, J. M. Keith, S. A. Kozimor, W. W. Lukens, R. L. Martin, D. K. Shuh, S. C. E. Stieber, T. Tylisczcak, and X.-d. Wen, *J. Am. Chem. Soc.,* 2017, **139**, 18052-18064.